

Isospin splitting of nucleon effective mass and isospin effect in heavy-ion collisions

FENG Zhaoqing^{*}

Institute of Modern Physics, Chinese Academy of Sciences, Lanzhou 730000, China

Abstract Two different isospin splittings of nucleon effective mass in nuclear medium as the form of $m_n^* > m_p^*$ and $m_n^* < m_p^*$ have been implemented in an isospin and momentum dependent transport model. Their impacts on the isospin emission in heavy-ion collisions is investigated thoroughly. It is found that the yield ratios of energetic neutrons to protons squeezed out during the compression stage of two colliding nuclides are sensitive to the isospin splitting. The elliptic flows of free nucleons are also to be promising observables for extracting the nucleon effective mass splitting. Further experimental measurements are being expected, in particular at the CSR-CEE platform in Lanzhou. Several observables are proposed for constraining the density dependence of symmetry energy, such as the transverse flow difference of neutrons and protons, double ratios of n/p and π^-/π^+ , excitation functions of π^-/π^+ and K^0/K^+ .

Key words Isospin splitting, Nucleon effective mass, Collective flows, Symmetry energy

1 Introduction

It has been well known that the masses of neutron and proton are equal each other in vacuum (about 1 GeV), and the effective mass in nuclear matter or finite nuclei deviates from its vacuum value^[1,2]. Moreover, a splitting of neutron and proton effective mass exists in neutron-rich nuclear matter, which increases with the isospin asymmetry and nucleon density. Predictions of the mass splitting based on nuclear many-body theories differ widely. Based on the realistic nucleon-nucleon interactions, the Brueckner-Hartree-Fock (BHF) and Dirac-Brueckner-Hartree-Fock (DBHF) calculations predict a neutron-proton mass splitting of $m_n^* > m_p^*$ ^[3-6]. The models based on relativistic mean-field (RMF) theory give a contrary result after the inclusion of the isovector mesons ρ and δ ^[7-9]. The Skyrme-Hartree-Fock (SHF) predicts both splittings of $m_n^* > m_p^*$ and $m_n^* < m_p^*$ exist with different Skyrme parameters^[10]. More realistically, the mass splitting of neutron and proton has been constrained from the energy dependence of the Lane

(symmetry) potential by the nucleon-nucleus scattering experimental data, which moderately supports the mass splitting of $m_n^* > m_p^*$ ^[11]. Further constraints on the effective mass splitting from heavy-ion collisions are still necessary and its influence on reaction dynamics would be very interesting.

The knowledge of the density dependence of the nuclear symmetry energy is still poorly known, in particular at high baryon densities, but which has important application in nuclear physics itself and also in astrophysics. Heavy-ion reactions with neutron-rich beams provide a unique opportunity to explore the density-dependent symmetry energy in a broad domain of density. In this work, we present systematic investigations of the effective mass splitting of neutron and proton and its influence on reaction dynamics. An extraction of the high-density symmetry energy from the preequilibrium nucleon emission and meson production (π and K) is performed with an isospin and momentum dependent transport model^[12].

Supported by National Natural Science Foundation of China (NSFC) projects (No. 11175218) and the Advancement Society of Young Innovation of Chinese Academy of Sciences.

* Corresponding author. E-mail address: fengzhq@impcas.ac.cn

Received date: 2013-06-27

2 Model description

The time evolutions of the baryons and mesons in the process of two colliding partners under the self-consistently generated mean-field are governed by Hamilton's equations of motion. The Hamiltonian of baryons consists of the relativistic energy, the effective interaction potential and the momentum dependent part^[12]. A Skyrme-type momentum-dependent nucleon-nucleon force distinguishing isospin effect is parameterized and implemented in the Lanzhou Quantum Molecular Dynamics (LQMD) model, which leads to a splitting of nucleon effective mass in neutron-rich matter. A Skyrme-type form for the momentum-dependent potential in the Hamiltonian by distinguishing isospin effect is taken in the LQMD model, which is expressed as

$$U_{\text{mom}} = \frac{1}{2\rho_0} \sum_{\tau\tau'} C_{\tau\tau'} \iiint d\mathbf{p} d\mathbf{p}' d\mathbf{r} f_\tau(\mathbf{r}, \mathbf{p}) \times \left[\ln(\varepsilon(\mathbf{p} - \mathbf{p}')^2 + 1) \right]^2 f_{\tau'}(\mathbf{r}, \mathbf{p}') . \quad (1)$$

Here $C_{\tau\tau} = C_{\text{mom}}(1+x)$, $C_{\tau\tau'} = C_{\text{mom}}(1-x)$ ($\tau \neq \tau'$) and the isospin symbols τ (τ') represent proton or neutron. The sign of x determines different mass splitting of proton and neutron in nuclear medium, e.g. positive signs corresponding to the case of $m_n^* < m_p^*$. The parameters C_{mom} and ε were determined by fitting the real part of optical potential as a function of incident energy from the proton-nucleus elastic scattering data. In the calculation, we take the values of 1.76 MeV, 500 c^2/GeV^2 for C_{mom} and ε , respectively, which result in the effective mass $m/m=0.75$ in nuclear medium at saturation density for symmetric nuclear matter. The parameter x can be adjusted as the strength of the mass splitting, and the values of -0.65 and 0.65 are respective to the cases of $m_n^* > m_p^*$ and $m_n^* < m_p^*$. One can get the contribution of momentum-dependent interaction to symmetry energy for a cold nuclear with Fermi distribution for a phase-space density $f_\tau(\mathbf{r}, \mathbf{p}) = \rho_\tau(\mathbf{r}) \Theta(p_F(\tau) - |\mathbf{p}|) / (4\pi p_F^3(\tau) / 3)$ with a Fermi momentum $p_F(\tau) = \hbar(3\pi^2 \rho_\tau)^{1/3}$. The symmetry energy per nucleon in the LQMD model is composed of three parts, namely the kinetic energy, the local part and the momentum dependence of the potential energy as

$$E_{\text{sym}}(\rho) = \frac{1}{3} \frac{\hbar^2}{2m} \left(\frac{3}{2} \pi^2 \rho \right)^{2/3} + E_{\text{sym}}^{\text{loc}}(\rho) + E_{\text{sym}}^{\text{mom}}(\rho) . \quad (2)$$

After the inclusion of momentum dependent contribution, a density, isospin and momentum dependent single-nucleon potential is obtained as follows:

$$U_\tau(\rho, \delta, \mathbf{p}) = \alpha \frac{\rho}{\rho_0} + \beta \left(\frac{\rho}{\rho_0} \right)^\gamma + \frac{8}{3} g_\tau \left(\frac{\rho}{\rho_0} \right)^{5/3} + E_{\text{sym}}^{\text{loc}}(\rho) \delta^2 + \frac{\partial E_{\text{sym}}^{\text{loc}}(\rho)}{\partial \rho} \rho \delta^2 + E_{\text{sym}}^{\text{loc}}(\rho) \rho \frac{\partial \delta^2}{\partial \rho_\tau} + \frac{1}{\rho_0} C_{\tau\tau} \int d\mathbf{p}' f_\tau(\mathbf{r}, \mathbf{p}) \left[\ln(\varepsilon(\mathbf{p} - \mathbf{p}')^2 + 1) \right]^2 + \frac{1}{\rho_0} C_{\tau\tau'} \int d\mathbf{p}' f_{\tau'}(\mathbf{r}, \mathbf{p}) \left[\ln(\varepsilon(\mathbf{p} - \mathbf{p}')^2 + 1) \right]^2 \quad (3)$$

Here $\tau \neq \tau'$, $\partial \delta^2 / \partial \rho_n = 4 \delta \rho_p / \rho^2$, and $\partial \delta^2 / \partial \rho_p = -4 \delta \rho_n / \rho^2$. The nucleon effective (Landau) mass in nuclear matter of isospin asymmetry $\delta = (\rho_n - \rho_p) / \rho$ with ρ_n and ρ_p being the neutron and proton density, respectively, is calculated through the potential as

$$m_\tau^* = m_\tau / \left(1 + \frac{m_\tau}{|\mathbf{p}|} \left| \frac{dU_\tau}{d\mathbf{p}} \right| \right) \text{ with the free mass } m_\tau \text{ at}$$

Fermi momentum $\mathbf{p} = \mathbf{p}_F$. Therefore, the nucleon effective mass only depends on the momentum-dependent term of the nucleon optical potential.

Figure 1 is a comparison of the momentum dependence of single-nucleon optical potential with the mass splittings of $m_n^* > m_p^*$ in the left window and $m_n^* < m_p^*$ in the right window for the hard and supersoft symmetry energies, respectively. One should note that a cross of neutron and proton single-nucleon potentials appears in the case of $m_n^* > m_p^*$ at high momentum, but which does not take place in the mass splitting of $m_n^* < m_p^*$ and a broader separation exists with increasing the nucleon momentum. The difference of single-particle potentials for both mass splitting affects the isospin emission in heavy-ion collisions, in particular, in the domain of high-baryon densities.

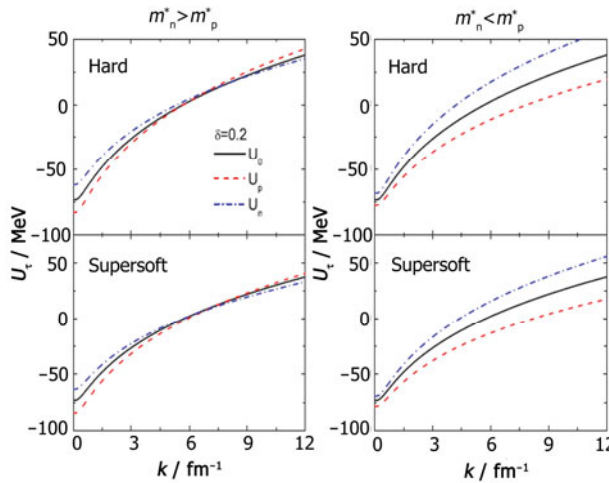


Fig.1 (Color online) Momentum dependence of single-nucleon optical potential for isospin symmetric matter ($\delta=0$) and neutron-rich matter ($\delta=0.2$) with the mass splittings of $m_n^* > m_p^*$ (left panel) and $m_n^* < m_p^*$ (right panel), respectively.

The scattering in two-particle collisions is performed by using a Monte Carlo procedure, in which the probability to be a channel in a collision is calculated by its contribution of the channel cross section to the total cross section. The primary products in nucleon-nucleon (NN) collisions in the region of 1A GeV energies are the resonances of $\Delta(1232)$, $N^*(1440)$, $N^*(1535)$ and the pions. We have included the reaction channels as follows:

$$\begin{aligned} NN &\leftrightarrow N\Delta, \quad NN \leftrightarrow NN^*, \quad NN \leftrightarrow \Delta\Delta, \\ \Delta &\leftrightarrow N\pi, \quad N^* \leftrightarrow N\pi, \quad NN \leftrightarrow NN\pi(s\text{-state}), \quad (4) \\ N^*(1535) &\rightarrow N\eta. \end{aligned}$$

At the considered energies, there are mostly Δ resonances which disintegrate into a π and a nucleon in the evolutions. However, the N^* yet gives considerable contribution to the energetic pion yields.

The strangeness is created as the secondary products in inelastic hadron-hadron collisions^[13,14]. We included the channels as follows:

$$\begin{aligned} BB &\rightarrow BYK, \quad BB \rightarrow BB\bar{K}, \quad B\pi \rightarrow YK, \\ B\pi &\rightarrow N\bar{K}, \quad Y\pi \rightarrow B\bar{K}, \quad B\bar{K} \rightarrow Y\pi, \quad (5) \\ YN &\rightarrow \bar{K}NN. \end{aligned}$$

Here the B strands for (N, Δ, N^*) and $Y(\Lambda, \Sigma)$, $K(K^0, K^+)$ and $\bar{K}(K^0, K^-)$. The elastic scattering between strangeness and baryons is considered through the channels of $K B \rightarrow K B$, $YB \rightarrow YB$ and $\bar{K} B \rightarrow \bar{K} B$. The charge-exchange reactions between the $K N \rightarrow K N$ and

$Y N \rightarrow Y N$ channels are included by using the same cross sections with the elastic scattering, such as $K^0 p \rightarrow K^+ n$, $K^+ n \rightarrow K^0 p$ etc. Correction of effective mass of kaons in nuclear medium on the elementary cross section is considered through the threshold energy, which results in the reduction of kaon and the enhancement of anti-kaon yields in heavy-ion collisions.

The evolution of mesons (here mainly pions and kaons) is also determined by a Hamiltonian. Here, the Coulomb interaction is considered for pion and kaon propagation. The kaon and anti-kaon energy in the nuclear medium is computed from the chiral Lagrangian. A repulsive kaon-nucleon (KN) potential and attractive antikaon-nucleon potential with the values of 25.5 MeV and -96.8 MeV are used in the model, which result in the effective mass with $m_K^* / m_K = 1.05$ and $m_{\bar{K}}^* / m_{\bar{K}} = 0.8$ at saturation baryon density.

3 Results and discussion

The preequilibrium nucleons in high-energy heavy-ion collisions are mostly produced during a compression stage of two colliding partners within a very short time. Therefore, the high-density information of nuclear phase diagram is expected to be extracted from the nucleons or light complex particles, which can be constrained from the longitudinal rapidity distributions and the azimuthal emissions. Shown in Fig.2 is a comparison of transverse emission ratios of neutron/proton within the rapidity selection of $|y/y_{\text{proj}}| < 0.25$ in the $^{197}\text{Au} + ^{197}\text{Au}$ reaction at the incident energy of 400A MeV for the near central ($b=1$ fm) and semi-central ($b=6$ fm) collisions, but with different mass splittings. One can see that the influence of the symmetry energy appears at low transverse momentum and the situation does not be changed with the mass splitting. A hard symmetry energy enforces a strongly repulsive force on neutrons in the high-density domain, furthermore, squeezes out more neutrons in the preequilibrium stage of dynamical evolution. From the negative contribution of the momentum-dependent interaction of $m_n^* > m_p^*$ to the potential part of the symmetry energy in Ref.[12], one notices that the momentum-dependent potential leads to an attractive force on neutrons, in

particular at high densities, which reduces the n/p yields at high transverse momentum. Opposite contributions take place and a flat distribution appears in the case of $m_n^* < m_p^*$. The spectrum of n/p has a slightly different structure with the results in Ref.[15] that is caused from the momentum dependent contribution of symmetry potential.

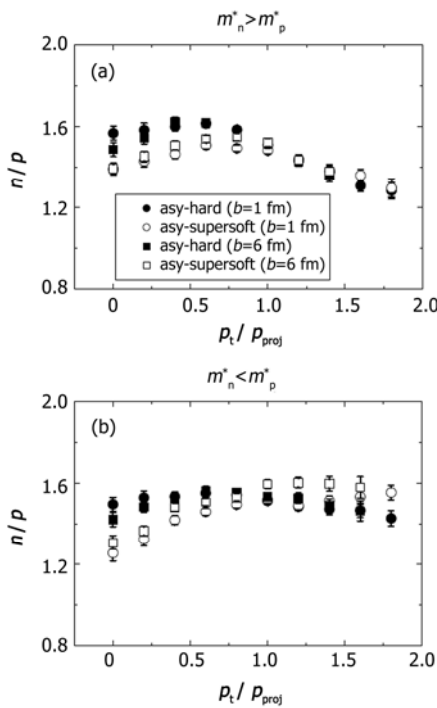


Fig.2 Transverse momentum distributions of neutron/proton within the rapidity bin $|y/y_{\text{proj}}| < 0.25$ in the $^{197}\text{Au} + ^{197}\text{Au}$ reaction at the incident energy of 400 MeV/nucleon for the near central ($b=1$ fm) and semi-central ($b=6$ fm) collisions with different mass splitting.

Collective flow has been verified as a nice approach to reconstruct the reaction plane and to study azimuthal correlation of the fireball formed in heavy-ion collisions. More sensitive observable can be seen from the flow difference between neutron and proton as shown in Fig.3. The $m_n^* > m_p^*$ case is always larger, in particular in the domain of high transverse momentum. Basically, the symmetry energy does not change the spectrum structure. We calculated the difference of neutron and proton directed flows as a function of rapidity distribution in the $^{197}\text{Au} + ^{197}\text{Au}$ collisions ($b=6$ fm) at the energy of 400 MeV with the hard and supersoft symmetry energies, but for the different mass splitting as shown in Fig.4. One can see that an anti-flow spectrum appears in both mass splitting in comparison with nucleon flows^[16,17].

Moreover, the supersoft symmetry energy gives a larger flow difference, in particular around the region of projectile (target) rapidity. The phenomena can not be influenced by changing different mass splitting. The flows of fast nucleon emissions would be a nice probe for extracting the high-density behavior of nuclear symmetry energy.

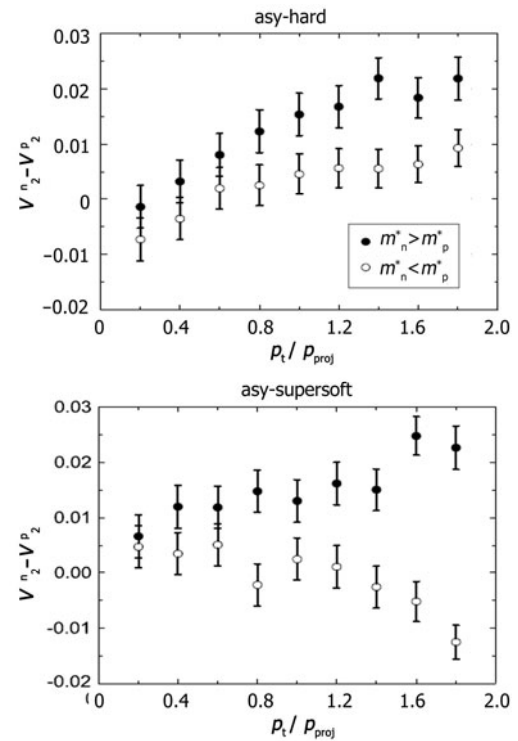


Fig.3 Comparison of the difference between neutron and proton elliptic flows with the rapidity bin $|y/y_{\text{proj}}| < 0.25$ for different mass splitting in semi-central $^{197}\text{Au} + ^{197}\text{Au}$ collisions.

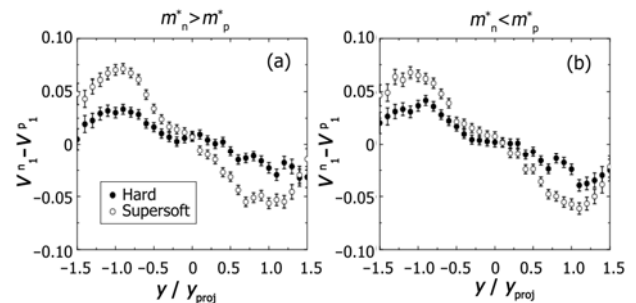


Fig.4 Transverse flow difference between neutrons and protons in semi-central $^{197}\text{Au} + ^{197}\text{Au}$ collisions at the energy of 400 MeV/nucleon with the hard and supersoft symmetry energies for different mass splittings of $m_n^* > m_p^*$ and $m_n^* < m_p^*$.

Kaon meson is produced at the early stage in heavy-ion collision and promptly emitted after production, which can get directly the information of

high-density phase diagram. A pronounced effect of the stiffness of symmetry energy on kaon production can be observed from the spectrum of isospin ratio. The isospin effects appear at deep subthreshold energies as shown in Fig.5. The in-medium potential slightly changes the K^0/K^+ value because of its influence on the kaon propagation and also on the charge-exchange reactions. At the considered energies, the channel of $N\Delta \rightarrow NYK$ contributes the main part for the kaon yields due to the larger production cross sections and the higher invariant energy, and the $NN \rightarrow NYK$ as well as $\pi N \rightarrow YK$ have about one third contributions. One notices that a hard symmetry energy always has the larger values of the isospin ratios than the supersoft case in the domain of subthreshold energies ($E_{th}(K)=1.58$ GeV).

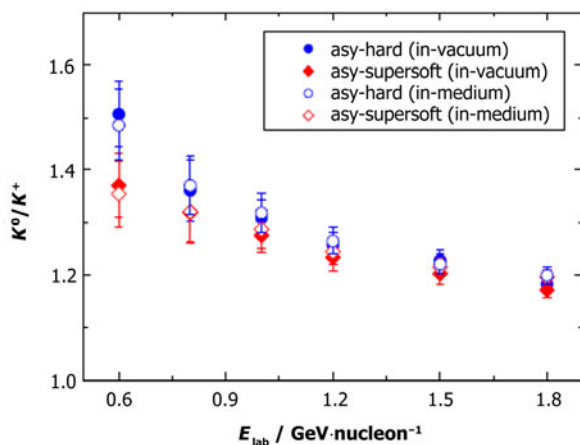


Fig.5 (Color online) Comparison of excitation functions of the K^0/K^+ yields for central $^{197}\text{Au}+^{197}\text{Au}$ collisions for the cases of hard and supersoft symmetry energies.

4 Conclusion

In summary, within the transport model (LQMD) we have investigated the impact of the momentum-dependent interaction on fast nucleon emissions in heavy-ion collisions. Two different mass splittings, i.e., $m_n^* > m_p^*$ and $m_n^* < m_p^*$, are chosen in the calculations. The momentum-dependent potential plays a significant role on the fast nucleon emissions. Specifically, the neutron/proton ratio at high transverse momenta is influenced, in which a flat

spectrum appears in the case of $m_n^* < m_p^*$. The elliptic flow difference between neutron and proton sensitively depends on the mass splitting, in particular at high transverse momenta. The neutron/proton ratio and the transverse flow difference of neutron and proton via transverse momentum distribution in the domain of mid-rapidity are sensitive to the stiffness of nuclear symmetry energy, which can be promising observables for extracting the high-density behavior of symmetry energy. The K^0/K^+ ratio of neutron-rich heavy system in the domain of subthreshold energies is also sensitive to the stiffness of nuclear symmetry energy.

References

- 1 Jeukenne J P, Lejeune A, Mahaux C. Phys Rep, 1976, **25**: 83–174.
- 2 Mahaux C, Bortignon P F, Broglia R A, *et al.* Phys Rep, 1985, **120**: 1–274.
- 3 van Dalen E N E, Fuchs C, Faessler A. Phys Rev Lett, 2005, **95**: 022302.
- 4 van Dalen E N E, Fuchs C, Faessler A. Phys Rev C, 2005, **72**: 065803.
- 5 Sammarruca F, Barredo W, Krastev P. Phys Rev C, 2005, **71**: 064306.
- 6 Zuo W, Bombaci I, Lombardo U. Phys Rev C, 1999, **60**: 024605.
- 7 Frick T, Gad K, Müther H, *et al.* Phys Rev C, 2002, **65**: 034321.
- 8 Hassaneen Kh S A and Müther H. Phys Rev C, 2004, **70**: 054308.
- 9 Liu B, Greco V, Baran V, *et al.* Phys Rev C, 2002, **65**: 045201.
- 10 Baran V, Colonna M, Greco V, *et al.* Phys Rep, 2005, **410**: 335–466.
- 11 Li B A. Phys Rev C, 2004, **69**: 064602.
- 12 Feng Z Q. Phys Rev C, 2011, **84**: 024610.
- 13 Feng Z Q and Jin G M. Phys Rev C, 2010, **82**: 044615.
- 14 Feng Z Q. Phys Rev C, 2011, **83**: 067604.
- 15 Li Q, Li Z, Soff S, *et al.* Phys Rev C, 2005, **72**: 034613.
- 16 Feng Z Q. Phys Lett B, 2012, **707**: 83–87.
- 17 Feng Z Q. Phys Rev C, 2012, **85**: 014604.